APEM journal

Advances in Production Engineering & Management
Volume 13 | Number 3 | September 2018 | pp 297–306
https://doi.org/10.14743/apem2018.3.291

ISSN 1854-6250
Journal home: apem-journal.org
Original scientific paper

An integral algorithm for instantaneous uncut chip thickness measuring in the milling process

Li, Y.[a], Yang, Z.J.[a], Chen, C.[b, *], Song, Y.X.[a], Zhang, J.J.[a], Du, D.W.[c]

[a]College of Mechanical Science and Engineering, Jilin University, Changchun, Jilin, P.R. China
[b]College of Engineering, China Agricultural University, Beijing, P.R. China
[c]Institution of Oceangraphic Instrumentation, Shandong Academy of Science, Qingdao, P.R. China

A B S T R A C T

Instantaneous uncut chip thickness (IUCT) calculation is an essential work for dynamic cutting force prediction accurately in milling process. This study presents an integral algorithm in polar coordinate system for measuring the thickness of transient uncut chip. The milling trajectory, cycloidal motion, is adopted in the formulation. Both milling continuity and cutter run-out are also considered in this model. The developed model offers a methodology for calculating the IUCT precisely. Furthermore, a series of simulations are carried out under different processing parameters. The results suggest that increasing both the feed per tooth and number of teeth can surge the width of IUCT slightly, but decrease with smaller cutter radius. The milling force simulations are validated by the experiment results measured in the reference and compared with classical approximate method, showing the proposed IUCT model providing good applications in instantaneous milling force predictions.

A R T I C L E I N F O

Keywords:
Milling;
Instantaneous uncut chip thickness;
Dynamic cutting forces;
Integral algorithm

**Corresponding author:*
chenchao2018@cau.edu.cn
(Chen, C.)

Article history:
Received 7 December 2017
Revised 29 July 2018
Accepted 24 August 2018

1. Introduction

Milling is an important processing method in the field of machining. Milling force that originates in the cutter–workpiece interface is an important factor that affects vibrations, milling efficiency, surface quality and the chatter stability of CNC tools [1-3]. Various analytical prediction models for cutting force have been established to improve the accuracy and reliability of milling force [4-6]. These models differ considerably, but the cutting force and IUCT are closely related [7, 8]. Besides, the force prediction accuracy is also important for monitoring of work conditions, such as tool life, surface roughness, even the machining stability of the milling process [9, 10]. Martellotti was first to use an approximated formula to calculate chip thickness. The simplified tooth path is considered as circular and lack of tooth eccentricity or tooth run-out [11]. The IUCT expression of the tooth path is $T_t(\alpha) = f_{rN} \cdot \sin\alpha$, where f_{rN} is feed per tooth and α is the instantaneous angular position of the tooth, which is widely used and researched [12, 13]. S. Spiewak then proposed an improved model of calculating IUCT in milling process. He facilitated stepwise and orderly increases in model sophistication until a desirable level of performance was achieved. The application results indicates that the speed, accuracy and reliability of monitoring and control potentially have been all improved, while the calculation process is rather complex and time consuming [14]. Another classical model is the one proposed by Li *et al*. in 2001. Instead of using a numerical method, they calculated the thickness of instantaneous uncut chip with Taylor's series by analyzing true tooth trajectories [15]. In Kumanchik's model, an analytic expression for uncut chip thickness in milling process was formulated while considering a series of impact factors, such as the cycloidal motion of teeth, run-out, and uneven teeth spacing [16]. Some people then expressed interest in the model through making improvements or modifications in the calculations. The main contribution of Ge Song and his co-authors is their investigation on the accurate positions of geometric points in the profile of IUCT with different level of cut width. This study also adopted the iterative algorithm to improve the accuracy of the thickness of uncut chip at the chip cross-section [17]. Chip thickness in circular interpolation was examined in 2008. Saï *et al.* found an opposing trend between chip thickness and the radius of circular trajectory. The regions or movements of the cutter should be also considered [18]. N. Grossi improved the trochoidal motion formula by introducing run-out values by two variables- the distance (d) between geometric centers of two adjacent cutters and the instantaneous cutter angle α [19]. However, the present methods for measuring IUCT ignored the true path shape of the cutter tooth. Most used models entail a circular tool-path approximation evenly. As mentioned earlier, cutting force is primarily a function of IUCT in an analytical cutting force approach. These simplified models could not achieve satisfied accuracy definitely. Besides, Milling is a continuous process and the approximate circumferential model considers the IUCT as discrete line that connects the tool center to the current tooth's cutting edge which fails to describe the transient chip formation and also limits the application scope of formulas.

This study introduces an integral algorithm in polar coordinate system for measuring the thickness of transient uncut chip. The milling cutter trajectory, cycloidal motion, is adopted in the novel formula, in which the IUCT is associated with feed rate per teeth, number of teeth and cutter radius. Both the effect of milling continuity and the cutter run-out are also considered in this method. Furthermore, different processing parameters are used to obtain a series of IUCT. The simulation milling forces are validated by the experiments and the classical method, showing the advantages and accuracy of using the new proposed method. The nomenclature is given in the Appendix A.

2. Milling tooth path and equation

Researchers investigated the path of cutter tip during milling. Most of them assumed the tooth path of cutting points as circular [14]. However, the true path shape of the cutter should be considered as a trochoid, which is a more reasonable approach [1, 15]. Fig. 1(a) describes movement in the direction of a straight line of the milling cutter. The radius of the cutter is assumed as r, where in the teeth are evenly distributed along the circumference. When the milling cutter is in clockwise rotation, the total teeth are labeled as $1,2,3,\ldots,i,\ldots,N$. The speed of motor spindle is given as n (r/min).

The feed rate of the workpiece is labeled as v_f (mm/min). Thus, milling feed rate can be calculated using the Eqs. 1 and 2 [20]:

$$v_f = f_{rN} \cdot N \cdot n \tag{1}$$

$$n = \frac{1000 \cdot v}{\pi \cdot D} \tag{2}$$

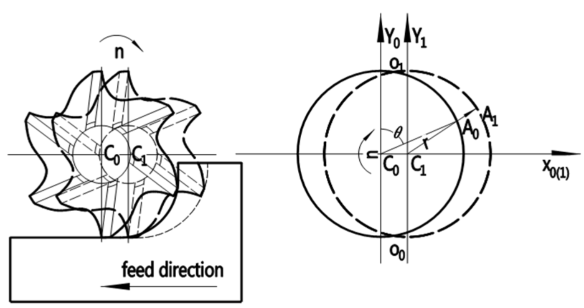

(a) (b)

Fig. 1 Model for milling cutter rotation: (a) milling along the liner direction; (b) milling tooth trajectory in Cartesian coordinate system

Variable f_{rN} is feed distance per tooth for one cycling, v is the rate of cutting, D is cutter diameter, which is twice the radius of the milling tool. The reasonable parameters can be given according to machining experience.

Cutter movement consists of its own rotation and rectilinear motion along the cutting direction. The feed distance of the tool center varies with the rotation angle of the cutter. Thus, feed distance for per angle f_{rad} (mm/rad) can be deduced from Eqs. 1 and 2:

$$f_{rad} = \frac{f_{rN} * N}{2\pi} \tag{3}$$

As shown in Fig. 1(b), the initial center of the tool is labeled as C_0, which coincides with the origin of the Cartesian coordinate system. The direction of the X-axis is opposite to the feed path of the workpiece and the Y-axis is normal to the X-axis. The Z-axis is perpendicular to the XOY coordinate plane and has the same direction as the cut depth. The equations represent the trajectories of arbitrary cutting point Q, namely *i* tooth. The tip of *i* + 1 tooth can be expressed as in [15]:

$$\begin{aligned} x_i &= f_{rz}\varphi_i + r\sin(\varphi_i - \omega t) \\ y_i &= r\cos(\varphi_i - \omega t) \end{aligned} \tag{4}$$

φ_i, the instantaneous angle of the cutter, is measured with the positive Y-axis as reference. Positive clockwise is the correct direction of the milling cutter, where $\varphi_i = \varphi_0 + (\mathrm{i} - 1)$. θ and φ_0 are the initial angle of the *i* tooth. The angle between *i* tooth and *i* +1 tooth can be calculated as:

$$\theta = 2\pi/N \tag{5}$$

3. Integral algorithm for instantaneous uncut chip thickness

3.1 Trajectory equation in polar form

Firstly, we transform the trajectory equation, deduced in Section 2, into the polar coordinate form. The polar point is coincident with origin C_0. The polar axis along the direction of X-axis positive can be found in the Cartesian coordinate system. Counterclockwise direction is assumed positive in polar angle α. The details of transformation are expressed as Eq. 6:

$$\begin{cases} x_i = \rho \cdot \cos\alpha \\ y_i = \rho \cdot \sin\alpha \end{cases} \tag{6}$$

The polar equation of the trajectory of *i* tooth can be represented by the following equation:

$$\rho_0^2 = r^2 \tag{7}$$

The polar equation of the route of *i* + 1 tooth can be written as Eq. 8:

$$(\rho_1 \cdot \cos\alpha - f_{rad} \cdot \varphi_i)^2 + (\rho_1 \cdot \sin\alpha)^2 = r^2 \tag{8}$$

Where ρ_0 and ρ_1 are respectively the polar radius of path *i* and *i* + 1 tooth, which are denoted as curve 'C_0A_0' and curve 'C_1A_1' in Fig. 1(b). We assume that $m = f_{rad} \cdot \varphi_i$ can be solved and simplified easily.

$$\rho_1 = m \cdot \cos\alpha \pm \sqrt{r^2 - (m \cdot \sin\alpha)^2} \tag{9}$$

It is obvious that feed distance is smaller than the cutter radius [13]. Therefore, we determine the following formula as reasonable when $m \ll r$:

$$m \cdot \cos\alpha - \sqrt{r^2 - (m \cdot \sin\alpha)^2} < 0 \tag{10}$$

Thus,

$$\rho_1 = m \cdot cos\alpha + \sqrt{r^2 - (m \cdot sin\alpha)^2} \tag{11}$$

where $\alpha \in (\alpha_0, \alpha_1)$ and α_0, α_1 are the polar angle formed at point A0 and A1, respectively, as shown in Fig. 1(b). The Y-axis positive axis is the polar axis where the teeth is cut into and cut out from the workpiece.

3.2 Analytical equation based on integral algorithm

Each cutter tooth is periodically engaged in the workpiece during the milling process. Thus, the IUCT is determined by the shape of two adjacent teeth trajectory when the milling process keeps steady, as shown in Fig. 2(a). The cuttings produced by each tooth are continuous and shaped by the cutting teeth. Chip thickness varies with instantaneous position angle in the cutting plane and the trajectories of the milling cutter [16]. According to the transformation and discussion in Section 3.1, Eqs. 7 and 11 represented the milling trajectories of the cutter tip attached to two adjacent teeth in the polar coordinate system. To improve calculation accuracy, the continuity of each milling tooth in one cycle should not be ignored. The uncut chip region between two adjacent teeth is divided into small regions, as shown in Fig. 2(b).

(a) Shape of two adjacent teeth trajectory (b) Micro-unit of definite integral in polar system

Fig. 2 Micro-unit of definite integral for true milling trajectory

The milling field is taken as the microcell unit and labeled as ΔS for ease of calculation. ΔS can be expressed by Eq. 12:

$$\Delta S = \Delta S_1 - \Delta S_0 \tag{12}$$

Following unit milling angleα_k, the area is taken as micro-unit of the definite integral. Eq. 13 can be described according to the area equation of the curved fan:

$$S = \lim_{\Delta\alpha_k \to 0} \sum_{k=1}^{n} \left(\frac{1}{2}\rho_1^2 \Delta\alpha_k - \frac{1}{2}\rho_0^2 \Delta\alpha_k \right) \tag{13}$$

Thus,

$$S = \int_{\delta_1}^{\delta_2} \left(\frac{1}{2}\rho_1^2 - \frac{1}{2}\rho_0^2 \right) d\alpha \tag{14}$$

where $\delta_1 \in \left(\frac{\alpha_0 \cdot 180°}{\pi}, \frac{\alpha_1 \cdot 180°}{\pi} \right)$ and $\delta_2 = \delta_1 + 1°$. The aim is to balance the calculation efficiency and accuracy. As written and discussed in the preceding section, the uncut chip area in the milling plane can be calculated using Eq. 14, which fully considers the continuity and trochoid of each tooth path. The uncut chip area can be calculated through Eq. 15:

$$S = \frac{m^2}{2} \cdot \int_{\delta_1}^{\delta_2} cos(2 \cdot \alpha)\, d\alpha + m \cdot \int_{\delta_1}^{\delta_2} cos\alpha \cdot \sqrt{r^2 - (m \cdot sin\alpha)^2}\, d\alpha \tag{15}$$

where angle α is measured with its polar axis along the direction of *X*-axis positive. The above equation is transformed into connect the instantaneous angle of cutterφ_i and the area of uncut chip thickness, where

$$\alpha = \begin{cases} \frac{\pi}{2} - \varphi_i, & 0 < x < \frac{\pi}{2} \\ -(\varphi_i - \frac{\pi}{2}), & \frac{\pi}{2} \le x < \pi \end{cases} \tag{16}$$

The definite integral expression in $\varphi_i$is takenas integration variable:

$$S = \frac{m^2}{2} \cdot \int_{\delta_1}^{\delta_2} cos(2 \cdot \varphi_i)\, d\varphi_i - m \cdot \int_{\delta_1}^{\delta_2} sin\varphi_i \cdot \sqrt{r^2 - (m \cdot cos\varphi_i)^2}\, d\varphi_i \tag{17}$$

Given that the instantaneous angle of cutter$\varphi_i$varies in small range, the corresponding arc length and radius can be regarded as approximately vertical. Thus, the shape of the integral section can be assumed as rectangle. The arc length for per radian can be calculated by Eqs. 18 and 19:

$$l_1 = \frac{\pi \cdot r}{180} \tag{18}$$

$$l_2 = \int_{\delta_1}^{\delta_2} \sqrt{\rho(\alpha)^2 + \overline{\rho(\alpha)}^2}\, d\alpha \tag{19}$$

where l_1 and l_2 represent per unit angle arc length of trajectory C_0 and C_1, respectively. Several milling parameters are adopted, shown in Fig. 3, to research length variation with rotation angle.

The length of milling path arc for each unit has a small range when specific milling parameters are given according to the Eqs. 18 and 19. The radius of the cutter significantly affects the arc length of milling path, as shown in Figs. 3(b) and 3(c).Thus, the mean value calculated according to specific radius is reasonable. The variation of uncut chip thickness with feed distance is 0.1 and 0.2. The upper and lower extremes of arc length obtained by Eq. 19 are used for calculation. Thus, the arc length mean value is employed in the calculation to improve the universality and accuracy of the proposed equation. The final expression of the uncut chip thickness is given as:

$$T_n(\alpha) = \frac{S}{\bar{l}} \tag{20}$$

$$\bar{l} = \frac{l_1 + l_2}{2} \tag{21}$$

S is integral area for per unit angle expressed as Eq. 17. The corresponding milling force based on the proposed analytical equation is deduced and calculated in the following section for the model verification.

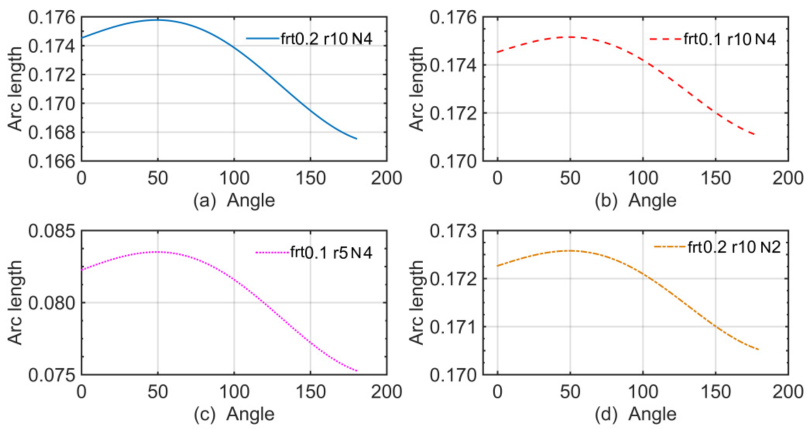

Fig. 3 Arc length for per milling unit with different milling parameters:
(a) f_{rt} = 0.2 mm/tooth, r = 10 mm, N = 4; (b) f_{rt} = 0.1mm/tooth, r = 10 mm, N = 4;
(c) f_{rt} = 0.1 mm/tooth, r = 5 mm, N = 4; (d) f_{rt} = 0.2 mm/tooth, r = 10 mm, N =2

4. Milling force calculation based on ICUT

The dynamic cutting force, according to the analytical mode proposed in reference [13], can be expressed as follows:

$$\begin{cases} F_{tj} = K_{tc}t(\alpha)z + K_{te}z \\ F_{rj} = K_{rc}t(\alpha)z + K_{re}z \\ F_{aj} = K_{ac}t(\alpha)z + K_{ae}z \end{cases} \tag{22}$$

where z is the contact length of cutting edge. During the milling process, both the shearing force of the primary shear zone and the rubbing force of the tertiary deformation zone exist. The milling force results depend on the instantaneous uncut chip thickness on the one hand, and on the other hand, material shear characteristics and the workpiece surface friction status are also closely related. The IUCT, $t(\alpha)$, can be calculated as the integral algorithm proposed in Section 3. The specific cutting force coefficients, $K_{ic}(i = t/r/a)$ and $K_{ie}(i = t/r/a)$in the equation, are determined by the average cutting force correction test [21].

The Eq. 22 can be mapped along the X, Y, and Z-directions in the Cartesian coordinate system using the following matrix transition:

$$\begin{pmatrix} dF_X \\ dF_Y \\ dF_Z \end{pmatrix} = \begin{pmatrix} -\cos\alpha & -\sin\alpha & 0 \\ \sin\alpha & -\cos\alpha & 0 \\ 0 & 0 & 1 \end{pmatrix} \begin{pmatrix} dF_{tj} \\ dF_{rj} \\ dF_{aj} \end{pmatrix} \tag{23}$$

The cutting force calculation process can be seen in following flowchart, Fig. 4. The computer programs in Matlab R2012b are carried out to obtain the specific milling force in direction $X/Y/Z$ in the following section.

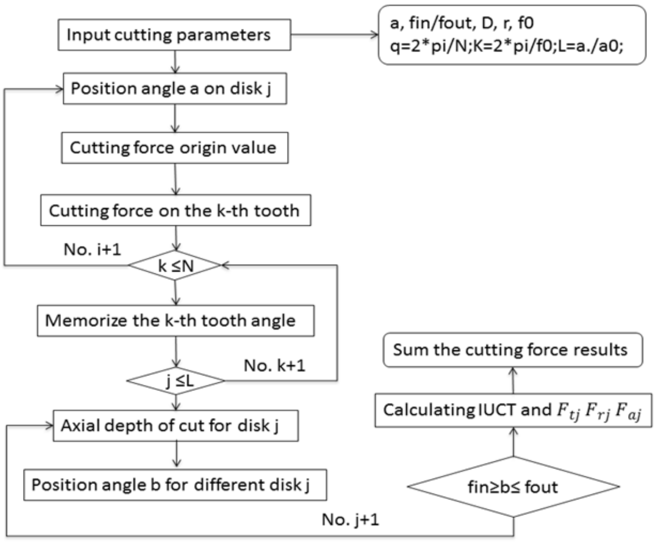

Fig. 4 Cutting force calculation flowchart

5. Results and discussion

5.1 Simulation and experiment analysis

Fig. 5 shows the measured milling forces in reference [21] and the simulations with the proposed integral method for a validation. The comparisons display that the trend of milling forces is roughly same in direction X, Y and Z. The chosen cutting conditions are listed in Table 1.

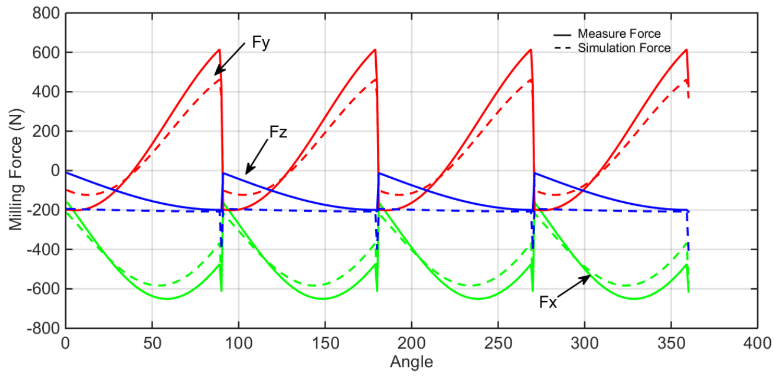

Fig. 5 Measured (from Yucesan and Altintas [21]) and predicted cutting forces for half immersion milling; N = 4, f_{rt} = 0.051 mm/tooth, a_p = 5.08 mm, v = 30 m/min

Table 1 Cutting conditions for single flute

Item	Parameter
Spindle speed	2500 rev/min
Cutting rate	30 m/min
Feed rate per teeth	0.051 mm/tooth
Depth of cut	5.08 mm
Cutter diameter	100 mm
Number of teeth	4
Helix angle	30°
Rake angle	10°
Material	AI 7050
Cutting force coefficients	In reference [21]

The measured forces from the reference are slightly larger than the calculations. It is suspect that the differences come from the specific cutting force coefficients which have large impacts on the simulations. During the milling process, cutting forces were generated from shearing force coming from chip formation and ploughing force at the flank of the cutting edge which are two main components of the cutting force coefficients [11, 19].

Thus, some specific milling tests should be carried out for comparisons when conditions permitted. In this work we just chose several specific cutting force coefficients for a comparison. Both the shear and edge cutting force coefficients are assigned according to the references [12, 21]. The developed integral IUCT model is used for milling force calculation compared with the results obtained by the approximate model $T_t(\alpha) = f_{rN} \sin \alpha$ with one single flute, as shown in Fig. 6.

The specific cutting condition is list in Table 2. The milling force with proposed integral model in X/Y/Z directions does not conform to those with approximate model through the whole cutting range, especially the milling force in horizontal machining surface. It is noted that the forces in the direction of X and Y are affected by the cutter tooth trajectory obviously. It is supposed that the trochoid motion of the tooth path causes a phase lag in the IUCT [15]. The maximum appears at 117°, not at 90°, where the milling force peak, in the *X*-direction, is about 250 N which is slightly larger than that calculated by approximate model. The integral algorithm reflects the continuity of milling process that is considered as the reason why the values are different at specific rotation angle. The proposed integral model for milling force prediction has good accuracy. In particular, it provides a better reference for predicting the rotation angle location of the maximum cutting force. While there are fine distinctions in Z direction and the fluctuations are also very little. It is suggested that cutting force in Z direction does nothing but depth of cut. However, the proposed integral equation ignores the effect of angle at cutting in and cutting out position. The milling force at 0° and 180°may not be accurate enough during the milling process. In addition, the analytic equation merely considers feeding movement as a straight line. But other milling conditions are not included such as the cutter centre follows a circular motion. The variation of IUCT may differ, as well as the calculation model, which should be explored further.

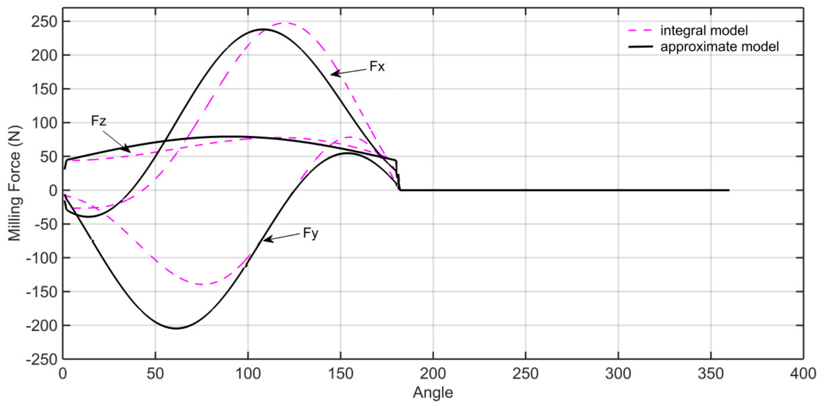

Fig. 6 Comparison of milling force results with different calculation models

Table 2 Cutting conditions for single flute

Item	Parameter
Cutting speed (m/min)	100m/min
Feed rate per teeth (mm/z)	0.06mm/tooth
Depth of cut(mm)	2mm
Cutter diameter(mm)	16mm
Number of teeth	1
Helix angle	0°
Rake angle	6°
Material	AISI 1045
Cutting force coefficients	In reference [12]

5.2 Effect of milling parameters on chip thickness

A variety of milling parameters, such as number of teeth, feed distance per tooth and milling cutter radius, are included in the analytical equation, which have a significant impact on the thickness of instantaneous uncut chip. Thus, in the following section the influence of the parameters is analysed. The results are shown in Fig. 7 and Fig. 8. Fig. 7(a) shows that when the feed rate for per tooth increases from 0.1 mm to 0.2 mm, the IUCT increases at the same time.

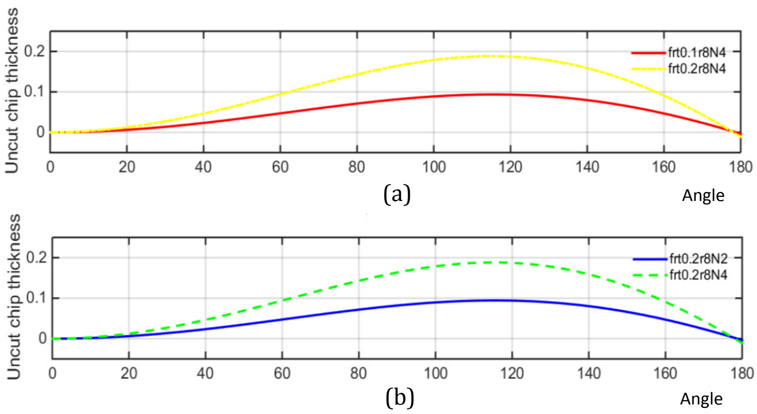

Fig. 7 (a) Effect of different feeding distance on uncut chip thickness (f_{rt} = 0.1 mm/tooth and 0.2 mm/tooth, *r* = 8 mm, *N* = 4); (b) Effect of different number of tooth on uncut chip thickness (f_{rt}= 0.2 mm/tooth, *r* = 8 mm, *N* = 2/4)

The width value of IUCT becomes bigger with more cutter teeth, as shown in Fig.7 (b). It is believed that this mainly comes from more teeth milling simultaneously, which induce in thermo-visco-plastic strength changes between adjacent teeth in the material. It can be deduced that it is in favour of micro milling process and improving roughness of the machined surface with multi-teeth cutter.

Fig. 8 shows the effect of cutter radius on the IUCT obtained by simulating under different radius. It is shown that the ICUT decrease when the cutter radius increase from 5 mm to 8 mm. It is supposed that small radius tools could improve the metal removing rate that is more suitable for machining precise part with small volume. It is noticeable that the results in Figs. 7 and 8 show that the maximum value of the IUCT appears at the rotation angle of 117° approximatively, which are consistent with the milling force results described in Fig. 6.

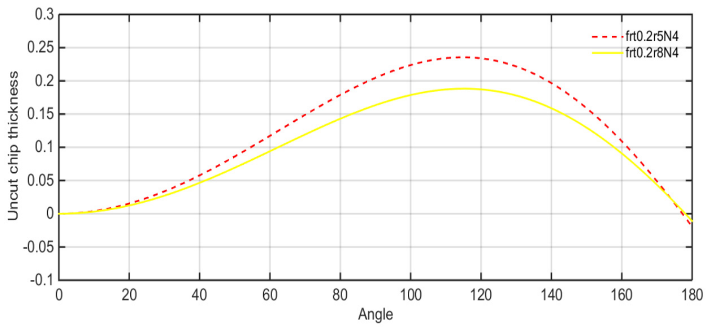

Fig. 8 Effect of different radius of milling cutter on uncut chip thickness (f_{rt} = 0.2mm/tooth, *r* = 5 mm and 8 mm, *N* = 4)

6. Conclusion

A method based on polar integral algorithm for calculating the thickness of transient uncut chip thickness is proposed for the cutting force predictions in milling process. The analytical equation is also suitable for engineering application. The main findings of the research:

- True milling trajectory considered as trochoid motion was established in the polar coordinates. Both milling continuity and milling trajectory are considered when developing a new model for IUCT calculations. The new developed model offers a methodology for calculating the IUCT precisely.
- The milling forces obtained by experiment in reference [21] and simulations with the developed IUCT model are compared in the paper. The integral model proves to be more reasonable in terms of the location where the peak appears. Results indicate that the outcomes followed by the polar integral algorithm are close to the reality.
- Different process parameters are simulated and compared according to the results calculated by proposed model. The comparisons suggest that increasing both the feed per tooth and number of teeth can surge the width of IUCT slightly, but decrease with smaller cutter radius.

Acknowledgement

The authors would like to express their acknowledgment to National Science and Technology Major Project (2016ZX04004007), China Postdoctoral Science Foundation (2017M621203) and Science and Technology Project in Education Department of Jilin Province (JJKH20180133KJ).

References

[1] Omar, O.E.E.K., El-Wardany, T., Ng, E., Elbestawi, M.A. (2007). An improved cutting force and surface topography prediction model in end milling, *International Journal of Machine Tools and Manufacture,* Vol. 47, No. 7-8, 1263-1275, doi: 10.1016/j.ijmachtools.2006.08.021.

[2] Matsubara, A., Ibaraki, S. (2009). Monitoring and control of cutting forces in machining processes: A review, *Monitoring and Control of Cutting Forces in Machining Processes,* Vol. 3, No. 4, 445-456, doi: 10.20965/ijat.2009.p0445.

[3] Mwinuka, T.E., Mgwatu, M.I. (2015). Tool selection for rough and finish CNC milling operations based on tool-path generation and machining optimisation, *Advances in Production Engineering & Management*, Vol. 10, No. 1, 18-26, doi: 10.14743/apem2015.1.189.

[4] Milfelner, M., Cus, F., Balic, J. (2005). An overview of data acquisition system for cutting force measuring and optimization in milling, *Journal of Materials Processing Technology,* Vol. 164-165, 1281-1288, doi: 10.1016/j.jmatprotec.2005.02.146.

[5] Liu, X.-W., Cheng, K., Webb, D., Luo, X.-C. (2002). Improved dynamic cutting force model in peripheral milling. Part I: Theoretical model and simulation, *The International Journal of Advanced Manufacturing Technology,* Vol. 20, No. 9, 631-638, doi: 10.1007/s001700200200.

[6] Ikua, B.W., Tanaka, H., Obata, F., Sakamoto, S. (2001). Prediction of cutting forces and machining error in ball end milling of curved surfaces -I theoretical analysis, *Precision Engineering,* Vol. 25, No. 4, 266-273, doi: 10.1016/S0141-6359(01)00077-0.

[7] Qu, S., Zhao, J., Wang, T., Tian, F. (2015). Improved method to predict cutting force in end milling considering cutting process dynamics, *The International Journal of Advanced Manufacturing Technology,* Vol. 78, No. 9-12, 1501-1510, doi: 10.1007/s00170-014-6731-5.

[8] Han, Z., Jin, H., Fu, H. (2015). Cutting force prediction models of metal machining processes: A review, In*: Proceedings of 2015 International Conference on Estimation, Detection and Information Fusion (ICEDIF),* Harbin, China, 323-328, doi: 10.1109/ICEDIF.2015.7280216.

[9] Gradišek, J., Kalveram, M., Weinert, K. (2004). Mechanistic identification of specific force coefficients for a general end mill, *International Journal of Machine Tools and Manufacture,* Vol. 44, No. 4, 401-414, doi: 10.1016/j.ijmachtools.2003.10.001.

[10] Saric, T., Simunovic, G., Simunovic, K. (2013). Use of neural networks in prediction and simulation of steel surface roughness, *International Journal of Simulation Modelling,* Vol. 12, No. 4, 225-236, doi: 10.2507/IJSIMM12(4)2.241.

[11] Martellotti, M.E. (1945). An analysis of the milling process, Part II: Down milling, *Transactions of ASME,* Vol. 67, No. 4, 233-251.

[12] Gonzalo, O., Beristain, J., Jauregi, H., Sanz, C. (2010). A method for the identification of the specific force coefficients for mechanistic milling simulation, *International Journal of Machine Tools and Manufacture,* Vol. 50, No. 9, 765-774, doi: 10.1016/j.ijmachtools.2010.05.009.
[13] Budak, E., Altintaş, Y., Armarego, E.J.A. (1996). Prediction of milling force coefficients from orthogonal cutting data, *Journal of Manufacturing Science and Engineering*, Vol. 118, No. 2, 216-224, doi: 10.1115/1.2831014.
[14] Spiewak, S. (1995). An improved model of the chip thickness in milling, *CIRP Annals,* Vol. 44, No. 1, 39-42, doi: 10.1016/s0007-8506(07)62271-9.
[15] Li, H.Z., Liu, K., Li, X.P. (2001). A new method for determining the undeformed chip thickness in milling, *Journal of Materials Processing Technology,* Vol. 113, No. 1-3, 378-384, doi: 10.1016/S0924-0136(01)00586-6.
[16] Kumanchik, L.M., Schmitz, T.L. (2007). Improved analytical chip thickness model for milling, *Precision Engineering,* Vol. 31, No. 3, 317-324, doi: 10.1016/j.precisioneng.2006.12.001.
[17] Song, G., Li, J., Sun, J. (2013). Approach for modeling accurate undeformed chip thickness in milling operation, *The International Journal of Advanced Manufacturing Technology,* Vol. 68, No. 5-8, 1429-1439, doi: 10.1007/s00170-013-4932-y.
[18] Saï, L., Bouzid, W., Zghal, A. (2008). Chip thickness analysis for different tool motions: For adaptive feed rate, *Journal of Materials Processing Technology*, Vol. 204, No. 1-3, 213-220, doi: 10.1016/j.jmatprotec.2007.11.094.
[19] Grossi, N., Sallese, L., Scippa, A., Campatelli, G. (2015). Speed-varying cutting force coefficient identification in milling, *Precision Engineering,* Vol. 42, 321-334, doi: 10.1016/j.precisioneng.2015.04.006.
[20] Fu, G. (2000). Basic knowledge of metal cutting, In: Shi, Q.F, Wang, L. (eds.), *Metal cutting manual*, (Third edition), Shanghai Science and Technology Press, Shanghai, 1-31, (in Chinese).
[21] Altintas, Y. (2012). *Manufacturing automation: Metal cutting mechanics, machine tool vibrations, and CNC design,* (Second edition), Cambridge University Press, New York, USA, doi: 10.1017/CBO9780511843723.
[22] Moufki, A., Dudzinski, D., Le Coz, G. (2015). Prediction of cutting forces from an analytical model of oblique cutting, application to peripheral milling of Ti-6Al-4V alloy, *The International Journal of Advanced Manufacturing Technology,* Vol. 81, No. 1-4, 615-626, doi: 10.1007/s00170-015-7018-1.
[23] Armarego, E.J.A., Deshpande, N.P. (1993). Force prediction models and CAD/CAM software for helical tooth milling processes. II. Peripheral milling operations, *International Journal of Production Research,* Vol. 31, No. 10, 2319-2336, doi: 10.1080/00207549308956860.

Appendix A

Nomenclature

$T_t(\alpha)$	IUCT calculated by traditional model
φ	Instantaneous cutter angle
f_{rN}	Feed per tooth
r	Radius of milling cutter
N	Number of cutter tooth
n	Spindle speed
v_f	Feed rate of the workpiece
v	Rate of cutting
D	Cutter diameter
f_{rad}	Feed per rad
φ_i	Instantaneous cutter angle of the *i*-th tooth
θ	Cutter pitch angle
φ_0	Initial angle of the cutter
α	Instantaneous cutter angle in polar system
$\rho_i(i=0,1)$	Polar radius of trajectory for *i*-th tooth
ΔS	Microcell unit of milling field
α_k	Unit milling angle
$\delta_i(i=0,1)$	Lower and upper limit of integral
S	IUCT area of unit milling angle
$l_i(i=1,2)$	Arc length of trajectory per radian
$\bar{l}$	Mean value of arc length
$T_n(\alpha)$	IUCT calculated by proposed integral model
z	Cutting edge contact length
$K_{ic}(i=t/r/a)$	Tangential/radial/axial shearing force coefficients
$K_{ie}(i=t/r/a)$	Tangential/radial/axial edge force coefficients
a_P	Depth of cut
$dF_i(i=x/y/z)$	Instantaneous cutting force in *X*-, *Y*- and *Z*-direction
fin/fout	Entry/ Exit angle